

## EDGE RADIATION AT SIBERIA-2 STORAGE RING

V.N. Korchuganov, N.V. Smolyakov<sup>#</sup>, N. Yu. Svechnikov,  
RRC Kurchatov Institute, Moscow 123182, Russia.

### Abstract

At the present time an edge radiation generated by a relativistic electron beam at fringe fields of bending magnets in storage rings attracts widespread attention as a source of intensive ultraviolet and infrared radiation. In this report, we present the numerical simulation of flux and spatial distribution of edge radiation at Siberia-2 storage ring. It is shown that we will gain in intensity considerably for the radiation in a wide spectral range below 350 eV as compared with standard synchrotron radiation from regular part of bending field.

### INTRODUCTION

Electromagnetic edge radiation (ER) is produced by a relativistic charged particle in its passage through the fringe fields at the bending magnet edges. It was experimentally discovered in the late 1970s independently at Super Proton Synchrotron (SPS, CERN, Geneva) [1, 2] and at the electron synchrotron "Sirius" (INP, Tomsk, Russia) [3 - 5]. Notice that the nature of ER emitted by protons differs radically from ER emitted by electrons. Although ER of protons and electrons alike are more intensive than synchrotron radiation (SR) in the same bending magnet, ER from protons peaks at wavelengths much shorter than SR critical wavelength; contrastingly, ER from electrons peaks at wavelengths much longer than SR critical wavelength. This feature of ER in electron storage rings, once noted in the first theoretical works [4, 6], is widely discussed in the succeeding papers [7- 14]. Measurements of long-wave ER [15- 18] strengthened the belief that electron beam ER can be used as a bright source of electromagnetic radiation in the infrared - vacuum ultraviolet spectral range. Several infrared beam lines utilizing ER are now in operation [10, 15, 19].

The photons emitted at two adjacent bending magnets bounding a straight section, appear in the same narrow cone and are subsequently synchronized by the electron itself. This leads to the interference of ER. The interference manifests itself as additional oscillations in the radiation intensity distribution. This effect was observed experimentally [3-5] and should be included into simulations of ER distributions.

In this paper, spatial distributions and spectral fluxes of edge and synchrotron radiation at Siberia-2 electron storage ring are calculated. It is shown that ER can be used as a powerful source of long wavelength radiation in infrared - ultraviolet spectral range.

### SIBERIA-2 STORAGE RING

The magnetic system of Siberia-2 storage ring (electron beam energy of 2.5 GeV) consists of six mirror-symmetrical cells, each containing an achromatic bend

and a gap with a zero dispersion function [20]. The pole of each bending magnet is divided into two parts: the long one with the main field  $B=1.7$  T (bending radii of 490.54 cm) and a shorter one with a field  $B/4=0.425$  T. The shorter part of the magnetic pole adjoins to the long straight section. The distance between the down- and upstream edges of the bending magnets is 5340 mm, see Fig. 1. The measured fringe field is shown in Fig.2. Synchrotron radiation with 7.2 keV critical energy from the homogeneous 1.7 T field is extracted by  $10 \times 10$  mrad<sup>2</sup> beam lines. The radiation distributions were calculated at the following beam parameters [20]: 300 mA beam current,  $\sigma_x = 0.72$  mm,  $\sigma_x' = 0.11$  mrad,  $\sigma_z = 0.014$  mm,  $\sigma_z' = 0.056$  mrad. Since 0° port has a mask with entrance aperture 44 mm hor.  $\times$  16 mm vert. which is installed at 1580 mm downstream from the straight section, see Fig.1, ER distributions were calculated in the plane of this mask. The numerical evaluations are carried out with the package of computer codes SMELRAD (SiMulation of ELectromagnetic RADiation) [21]. Simulations include so-called "velocity term" and near-field effects. The program computes step by step the electron's trajectory in the given magnetic field, which should be prescribed in the input file with the magnetic field data. It makes possible to use experimentally measured data. Electron beam emittance effects are calculated via numerical convolution.

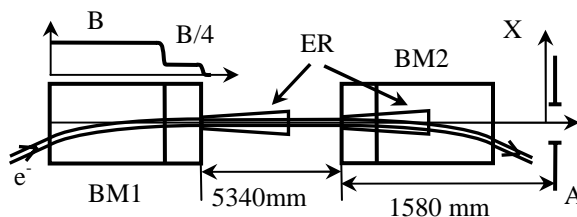


Fig. 1. Sketch of ER generation: BM1, BM2 - bending magnets, ER - edge radiation, A - aperture.

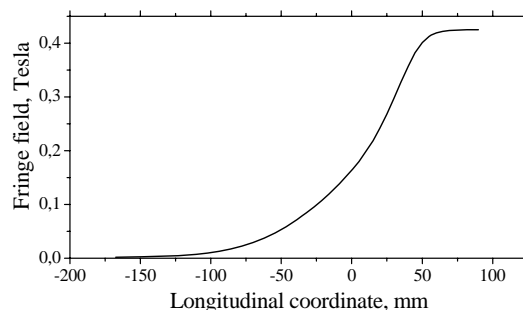


Fig. 2. Fringe field of Siberia-2 bending magnets.

<sup>#</sup>smolyakovnv@mail.ru

## RESULTS

Figure 3 displays the computed flux density in the Siberia-2 electron orbit plane 1580 mm downstream of a straight section, see Fig. 1. The flux density with 0.1 eV photon energy is plotted versus horizontal position  $X$ . The calculations were carried out for the electron beam with zero and nonzero emittance with 300 mA current. One can readily see that the nonzero emittance effects smooth out the fine interference oscillations. The distributions are substantially asymmetric about the straight section axis ( $X=0$ ) because of the relatively short distance from the screen to the straight section. It is apparent from Fig. 1 that the screen at  $X<0$  is illuminated mainly from the nearby BM2 bending magnet, while for  $X>0$  the screen is illuminated mainly from the distant BM1 bending magnet. The radiation distribution tends to the correspondent SR intensity as the distance from the straight section axis in the median plane  $|X|$  increases.

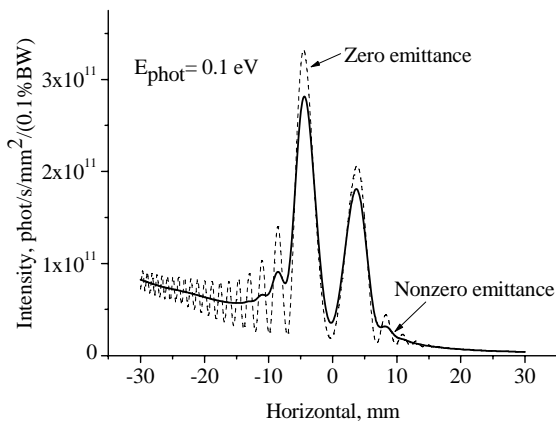


Fig. 3. Horizontal distributions of ER in the median plane.

The vertical cross sections of 0.1 eV ER distributions for different horizontal positions:  $X=0$  (straight section axis),  $X=-4.54$  mm (position of the main maximum in horizontal distribution, see Fig. 3) and  $X=-10$  mm are shown in Fig. 4.

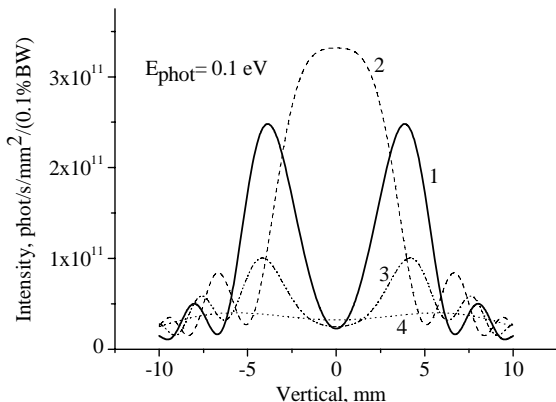


Fig. 4. Vertical distributions of ER for different  $X$ :  $X=0$  (1),  $X=-4.54$  mm (2),  $X=-10$  mm (3) and SR (4).

For comparison the SR vertical distribution from 1.7 T bending field is also plotted in the same figure (curve 4). It is easy to see that ER is much brighter than synchrotron radiation in long wavelength spectral range.

In Fig. 5, the ER and synchrotron radiation fluxes into  $10 \times 10$  mrad<sup>2</sup> solid angle centered on the straight section axis are shown. From this figure we notice that for a given aperture the flux of edge radiation far exceeds the synchrotron radiation flux for the photon energies less than 350 eV.

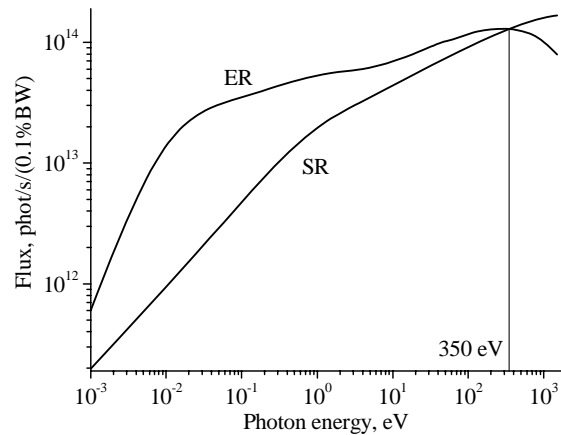


Fig. 5. ER and SR fluxes into  $10 \times 10$  mrad<sup>2</sup> solid angle.

It is worthy of note that application of ER considerably reduces thermal and radioactive load on beam line elements. Indeed, the generation of hard X-rays is suppressed along the straight section because the magnetic field is depressed at fringe regions. The total power generated in 1.7 Tesla bending field by the 300 mA electron beam into  $10 \times 10$  mrad<sup>2</sup> solid angle is equal to 340 W. At the same time the total power generated by this electron beam along straight section axis into  $28 \times 10$  mrad<sup>2</sup> (entrance aperture of mask, see Fig. 1) is equal to 54 W only.

## INFRARED BEAMLIN

At present, the project of a multipurpose infrared beamline is under development at the Siberia-2 storage ring. It will be equipped with a Fourier transform spectrometer and a microscope. The spectral range will span from 4 eV down to  $\sim 6$  meV for 3 experimental stations: UV-NearIR station at 4–1 eV, NearIR-Far IR station at  $5000\text{--}50$  cm<sup>-1</sup> and IR spectromicroscopy station at  $5000\text{--}500$  cm<sup>-1</sup>.

For the natural divergence  $\sigma_n$  of IR radiation from the bending magnet, evaluated by the known expression  $\sigma_n = 0,511 \times (\lambda/\lambda_c)^{1/3} \times (10^{-3}/E)$ , where  $E[\text{GeV}] = 2.5$ , the critical wavelength  $\lambda_c = 0.172$  nm for Siberia-2, and  $\sigma_n$  is given in [rad], one will obtain the  $\sigma_n$  values from 4 mrad to 22 mrad for the spectral range of  $5000\text{--}50$  cm<sup>-1</sup>. Therefore, to ensure the minimum losses at the first mirror in the Far-IR region, one must have a front-end with an aperture no less than  $22 \times 22$  mrad<sup>2</sup> (hor. $\times$ vert.).

The optical layout of the infrared K3.6 beamline and 3 stations of Siberia-2 are shown in Fig. 6, with side view (top) and top view (bottom). It can use ER from the straight section between two bending magnets. The beamline consists of a high vacuum part which is located inside the shield of Siberia-2, and a low vacuum part from the diamond window up to the hutches with experimental stations. The beamline is located in a horizontal plane.

The main advantage of the IR radiation concerns the possibility of beam transport to large distances with the help of metallic mirrors, plane and focusing with Al or Au film cover, due to almost 100% reflectivity at wavelengths  $\lambda > 0.5 \mu\text{m}$ . The first plane mirror with sizes about  $16 \times 16 \text{ cm}^2$ , water cooled, is located at 5300 mm from the radiation spot and after the  $30 \times 10 \text{ mrad}$  exit port, therefore the heat load will be several times smaller than the aforementioned 340 W for dipole radiation or 54 W for edge radiation. Besides accepting the radiation, the first mirror filters the VUV and X-ray radiation above 20 eV. The second elliptical mirror focuses the radiation onto the diamond window. The third refocusing mirror makes a parallel beam up to the location of the torroidal focusing mirror near each station.

The use of the edge radiation is known to have a more narrow divergence which will be especially important for Far-IR region.

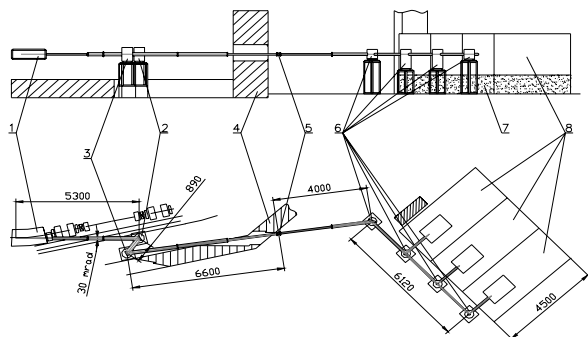


Fig.6. The infrared beamline and 3 stations: 1 – bending magnet with exit port of 30 mrad (horizontally), 2 – chamber of the first plane mirror, 3 – chamber of the elliptical focusing mirror, 4 – shielding, 5 – diamond window chamber, 6 – four chambers with torroidal focusing mirrors, 7 – concrete supporting block under the hutches, 8 – three experimental stations in hutches. The sizes are given in [mm].

## REFERENCES

- [1] R. Bossart, J. Bossier, L. Burnod et al., Nucl. Instr. and Meth. 164 (1979) 375.
- [2] R. Bossart, J. Bossier, L. Burnod et al., Nucl. Instr. and Meth. 184 (1981) 349.
- [3] M.M. Nikitin, A.F. Medvedyev, M.B. Moiseev, Sov. Tech. Phys. Lett. 5 (1979) 347.
- [4] M.M. Nikitin, A.F. Medvedyev, M.B. Moiseev, V.Ya. Epp, Sov. Phys. JETP 52 (1980) 388.
- [5] M.M. Nikitin, A.F. Medvedyev, M.B. Moiseev, IEEE Trans. Nucl. Sci. NS-28 (1981) 3130.
- [6] E.G. Bessonov, Sov. Phys. JETP 53 (1981) 433.
- [7] O.V. Chubar, N.V. Smolyakov, J. Optics (Paris) 24, No. 3 (1993) 117.
- [8] O.V. Chubar, N.V. Smolyakov, Proc. of the 1993 IEEE PAC Conf., Washington (1993) 1626.
- [9] K. J. Kim, Phys. Rev. Letters, 76, No. 3 (1995) 1244.
- [10] Y.-L. Mathis, P. Roy, B. Tremblay et al., Phys. Rev. Letters 80 (1998) 1220.
- [11] R.A. Bosch, Nucl. Instr. and Meth. A431 (1999) 320.
- [12] F. Meot, Part. Acceler. 62 (1999) 215.
- [13] R.A. Bosch, Nucl. Instr. and Meth. A454 (2000) 497.
- [14] R.A. Bosch, Nucl. Instr. and Meth. A492 (2002) 284.
- [15] T.E. May, R.A. Bosch and R.L. Julian, Proc. of the 1999 PAC Conf., New York (1999) 2394.
- [16] P. Roy, M. Guidi Cestelli, A. Nucara et al., Phys. Rev. Lett., 84(3) (2000) 483.
- [17] U. Schade, A. Roseler, E.H. Korte et al., Nucl. Instr. and Meth. A455 (2000) 476.
- [18] N.V. Smolyakov, A. Hiraya, Nucl. Instr. and Meth. A543 (2005) 51.
- [19] R.A. Bosch, R.L. Julian, R.W.C. Hansen et al., Proc. of the 2003 PAC Conf., Portland (2003) 929.
- [20] V.V. Anashin, A.G. Valentinov, V.G. Veshcherevich et al., Nucl. Instr. and Meth. A282 (1989) 369.
- [21] K. Shirasawa, N.V. Smolyakov, A. Hiraya, T. Muneyoshi, Nucl. Instr. and Meth. B199 (2003) 526.